# Study of A = 100–150 superdeformed mass region by using two-parameter formula

**Vidya DEVI**[1,*] , **Jagjit Singh MATHARU**[2]
[1]Department of Applied Sciences, IET Bhaddal, Ropar, India
[2]UIET, Panjab University, Chandigarh, India

**Abstract:** Empirical formulae of rotational spectra consisting two parameters, such as single-term energy formula, $E = aJ^b$ for spin $J$, and $ab$ formula, were used to study the different features of superdeformed band in A = 100–150 mass region nuclei. The nuclear kinematic and dynamic moment of inertia for the ground-state rotational bands were calculated for this purpose and both showed gradual rise with rotational frequency. The study of $\Delta I = 2$ staggering effects in the $\gamma$-ray energies, where the two sequences $J = 4i, 4i + 1$ and $J = 4i + 2$, $(i = 0, 1, \ldots)$ are bifurcated, was also done. We also calculated the variation of the gamma ray energies from a smooth reference using the fourth derivative of the gamma ray energies at a given spin. The excellent agreement between the observed and calculated transition energies are in good support of the two-parameter formula.

**Key words:** Superdeformed band, two parameter formula, staggering index, identical bands

## 1. Introduction

A superdeformed nucleus is a nucleus that is predicted to occur at specific magic numbers and at deformations corresponding to the integer ratios of the axes about 2:1:1. Generally, the normal deformation of the nucleus is about 1.3:1:1. Superdeformed structures have been found mostly in nuclei of the A = 150 and 240 mass regions, i.e. in the fission isomers low-spin states of elements in the actinide and lanthanide series. Recently, it has also been discovered in other mass regions, such as $A = 60, 80, 130$, and $190$. In the past few years, much effort has been devoted to study the underlying physics of superdeformed bands and other interesting facts and issues, such as the identical bands [1], $\Delta I = 1, 2$ staggering [2, 3] and the multipole correlation and exotic structure of nuclei [4].

A general understanding in the properties of superdeformed nuclei has been attained, but still there are open problems that need to be further studied. In this paper, we used empirical formula of rotational spectra consisting two parameters, i.e. single-term energy formula, $E = aJ^b$, and $ab$ formula, to study the different features of superdeformed band in A = 100–150 mass region.

The moment of inertia is one of the most significant quantities to characterize the nuclear rotational band. There are generally two kinds of moment of inertia ($\Im$) for illustrating the high-spin phenomena, i.e. the dynamic moment of inertia,

$$\Im^2 = \hbar \frac{dI_x}{d\omega} = \hbar^2 \left[ \frac{d^2 E}{dI_x^2} \right], \tag{1}$$

---

*Correspondence: vidyathakur@yahoo.co.in

and the kinematic moment of inertia,

$$\Im^1 = \frac{\hbar I_x}{\omega} = \hbar^2 I_x \left[ \frac{dE}{dI_x} \right]. \tag{2}$$

Usually, $\Im^1$ and $\Im^2$ are obtained from the intraband $\gamma$ transition energies by using the following formulae:

$$\Im^1(J-1) = \frac{(2J-1)}{E_\gamma(J)}, \tag{3}$$

$$\Im^2(J) = \frac{\hbar^2}{E_\gamma(J+2) - E_\gamma(J)}, \tag{4}$$

where $E_\gamma(J) \equiv E_\gamma(J \to J-2)$.

The expression for the rotational frequency $(\hbar\omega(I))$ of the nuclei is

$$\hbar\omega(I) = E_\gamma(J+1 \to J-1). \tag{5}$$

A number of idealized models are available to study and perceive the idea of nuclear structure that involves axial rotor [5], axial anharmonic vibrator [6], and $\gamma$-soft deformed nuclei [7, 8]. These models can be utilized for the prediction of $B(E2)$ values and energy sequences. The well-known expression for the ground-state band energy levels for rotational spectra is

$$E = \frac{\hbar^2}{2\Im(J)} J(J+1). \tag{6}$$

The three parametric simplest energy formula for the deformed nuclei is the Bohr–Mottelson energy expansion in terms of the power of $J(J+1)$, [9]

$$E = AJ(J+1) + B(J(J+1))^2 + CJ(J+1))^3. \tag{7}$$

Further, Holmberg and Lipas [10] observed that the moment of inertia of deformed nuclei ascends linearly with level energy, i.e.

$$\Im(J) = bE + a. \tag{8}$$

Substituting Eq. (8) in Eq. (6), they obtained the two-parameter $ab$ formula

$$E = a \left[ \sqrt{1 + bJ(J+1)} - 1 \right]. \tag{9}$$

The relation between $\Im$ and $E$ in rotational spectra for high and low spins is nonlinear, as described by Zeng et al. [11]. Rephrasing Eq. (8) and equating it with Eq. (5), Zeng et al. developed a new relation between $\Im$ and $E$

$$\Im = \frac{1}{2ab} \left( 1 + \sqrt{1 + \frac{2}{a}E} \right). \tag{10}$$

Using Eqs. (8) and (6), they developed a new expression for the energy called the $pq$ formula:

$$E = a \left( \left\{ p^2 + [p^4 + q^3]^{1/2} \right\}^{1/3} + \left\{ p^2 - [p^4 + q^3]^{1/2} \right\}^{1/3} \right),$$

where $p = bJ(J+1)/2$ and $q = bJ(J+1)/3$. Brentano et al. [12] further observed that $\Im$ depends upon the spin $(J)$ and energy $(E)$ by the relation

$$\Im = \Im_0(1 + aJ + bE). \tag{11}$$

By ignoring the energy term $bE$ in Eq. (10) and replacing it in Eq. (5), Brentano et al. derived a new formula containing two parameters called the soft rotor formula (SRF),

$$E = \frac{1}{\Im_0(1 + \alpha J)} J(J+1). \tag{12}$$

Gupta et al. [13, 14] replaced the concept of arithmetic mean of two terms used in the Bohr–Mottelson expression by the geometric mean to introduce a single-term energy formula for ground band level energies of soft rotor and called it power law,

$$E = aJ^b. \tag{13}$$

The index $b$ can be determined from the ratio,

$$R_J = E/E(2) = (J/2)^b, \tag{14}$$

for any spin $(J)$.

The paper is mainly divided into two parts. The first part contains a brief introduction of two- and three-parameter formula needed to study the properties of SD bands and also to calculate the transition energies, rotational frequencies $\hbar\omega$, and kinematic $\Im^1$ and dynamic $\Im^2$ moment of inertia. In the second part, we shall study other properties for SD bands such as identical bands and $\Delta I = 1$ staggering in $A \approx 100$–$150$ mass region.

## 2. Result and discussion

The systematic behaviors of $\Im^1$ and $\Im^2$ play a very important role in understanding the properties of superdeformed band. Figure 1 shows the variation of moment of inertia ($\Im^1$ and $\Im^2$) with $\hbar\omega$ for $^{151}$Tb(SD-2) and $^{151}$Dy(SD-2) nuclei. It can be observed that there is decrease in $\Im^1$ and $\Im^2$ values with the decrease $\hbar\omega$. Figure 2 shows gradual increase of $\Im^1$ and $\Im^2$ values with the increase $\hbar\omega$ for $^{194}$Hg(SD-1) and $^{194}$Pb(SD-1) nuclei. The data for Figures 1 and 2 have been taken from [15].

### 2.1. Identical bands in superdeformed nuclei

Over the past few years, there has been considerable interest in the study of SD rotational bands in consecutive even and odd mass nuclei having almost identical gamma transition energies [1]. More than thirty such SD rotational bands have been discovered in A = 150–190 mass region [16]. Several explanations were put forward assuming the existence of such identical bands to be the specific property of superdeformed states of nuclei. Casten et al. [17, 18] studied the low-spin identical bands in widely dispersed nuclei $^{156}$Dy-$^{180}$Os. There exists a simple correlation between the nuclei showing identical spectra and their valence proton $(N_p)$ and neutron $(N_n)$ boson numbers, which further provide the trace to understand the identical band phenomenon.

The occurrence of identical bands in adjacent even–even nuclei demands the symmetry in $\pm F_0$ values of moment of inertia in the F-spin multiplet besides identical $N_p N_n$ in the two bands. There are many examples of
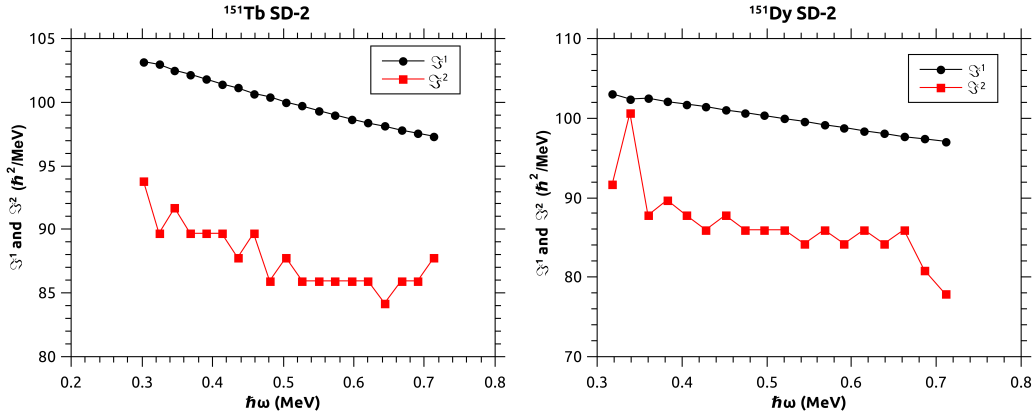
**Figure 1**. Experimental $\Im^1$ and $\Im^2$ $\left(\hbar^2/MeV\right)$ for $^{151}$Dy(SD-2) and $^{151}$Tb(SD-2) nuclei [15].
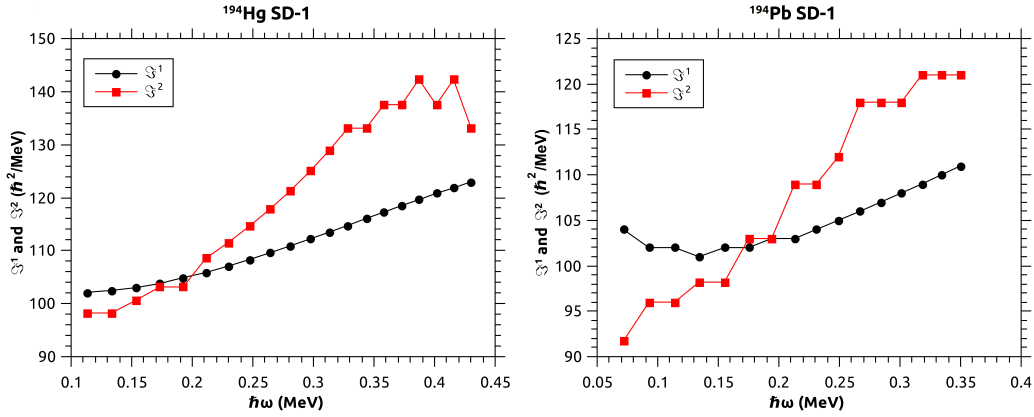


**Figure 2**. Experimental $\Im^1$ and $\Im^2$ $\left(\hbar^2/MeV\right)$ values for $^{194}$Hg(SD-1) and $^{194}$Pb(SD-1) nuclei [15].

identical bands that differ by two mass units and exist in pairs in the $A \approx 190$ mass region with the assumption of $^{192}$Hg as a doubly magic core. Generally, the degree of similarity can be seen when the difference between transition energies $\Delta E_\gamma$ for the identical pair of SD bands and the transition energy $E_\gamma$ is plotted [19]. It happens due to the alignment of angular momentum of a pair of nucleons that occupy high intrudes orbital and form the gradual disappearance of pairing correlations with increasing $\hbar\omega$.

Figure 3 shows the deviation of transition energy (keV) with $N_p N_n$ between the two states $^{194}$Hg(SD-1) and $^{194}$Pb(SD-1) nuclei having the same value of $\frac{N_p + N_n}{2} = 3.5$. The agreement between experimental spectra of these two nuclei is excellent. Similarly, Figure 4 shows the identical bands between $^{82}$Sr(SD) and $^{82}$Y(SD) having $N_p N_{=} 5, 4$ for $N_B = 9$. There is no violation of the symmetry in the spectra of these two SD band nuclei and the figure shows the staggering pattern.

## 2.2. Study of $\Delta I = 2$ staggering

Another interesting feature of SD nuclear bands is the $\Delta I = 2$ staggering sequences of states which differ by four units of angular momentum and are delocated with respect to each other. Many theoretical proposals were put forward for the possible clarification of the $\Delta I = 4$ bifurcation [20–22]. The variation of the $\gamma$-ray
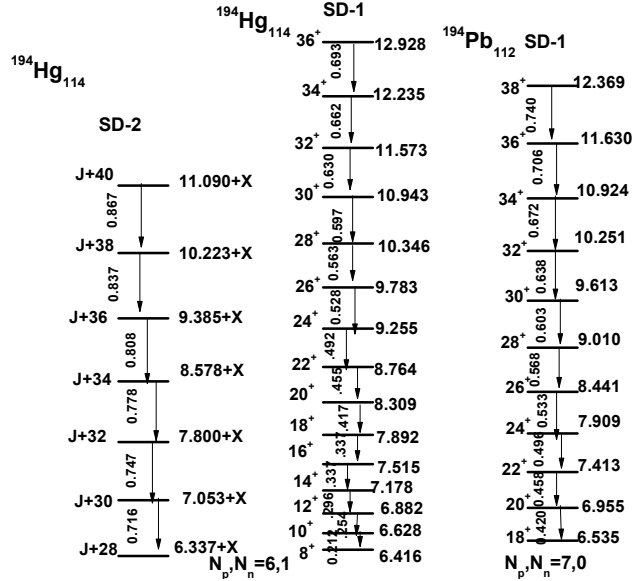
**Figure 3**. The deviation of transition energy (keV) with $N_p N_n$ between the two states for $N_B = 7$.
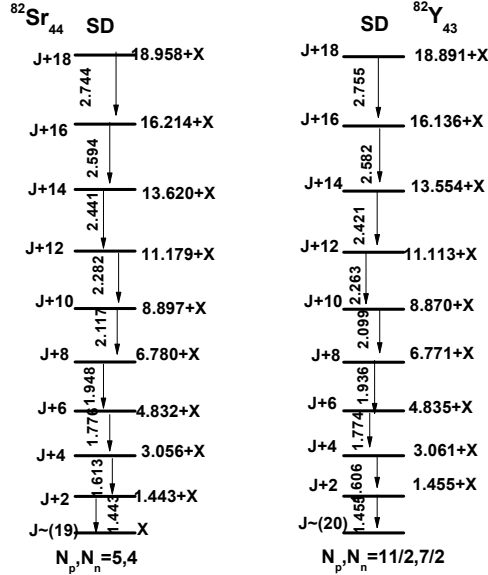


**Figure 4**. The deviation of transition energy (keV) with $N_p N_n$ between the two states for $N_B = 9$.

transition energies from the rigid rotor behavior can be calculated by the staggering quantity [23]

$$\Delta^4 E_\gamma(J) = \frac{1}{16} \left[ 6E_\gamma(J) - 4E_\gamma(J-2) - 4E_\gamma(J+2) + E_\gamma(J-4) + E_\gamma(J+4) \right]. \qquad (15)$$

The formula involves five consecutive transition energies $E_\gamma$ and hence called five-point formula.

We evaluated the staggering quantity $\Delta^4 E_\gamma$ and plotted it as a function of rotational frequency $\hbar\omega$ in Figure 5. The figure shows the staggering pattern $\Delta^4 E_\gamma$ for the $^{192}$Hg(SD-1), $^{194}$Hg (SD-1)(SD-2)(SD-3), and $^{194}$Pb(SD-1) band. For $^{192}$Hg(SD-1), the staggering values range from $-0.3$ to $0.3$ and as neutron
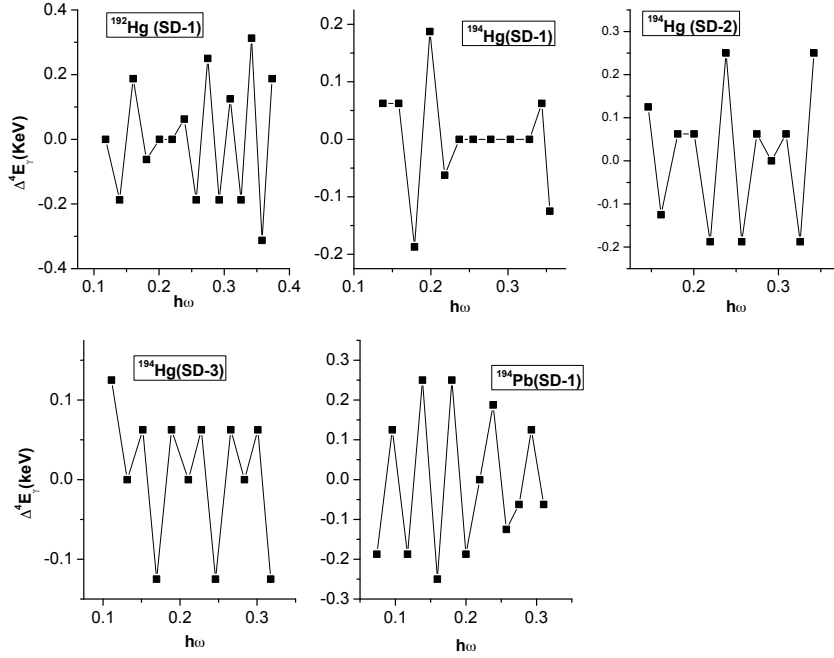
**Figure 5**. $\Delta^4 E_\gamma$ staggering pattern for the $^{192}$Hg(SD-1), $^{194}$Hg(SD-1)(SD-2)(SD-3), and $^{194}$Pb(SD-1).
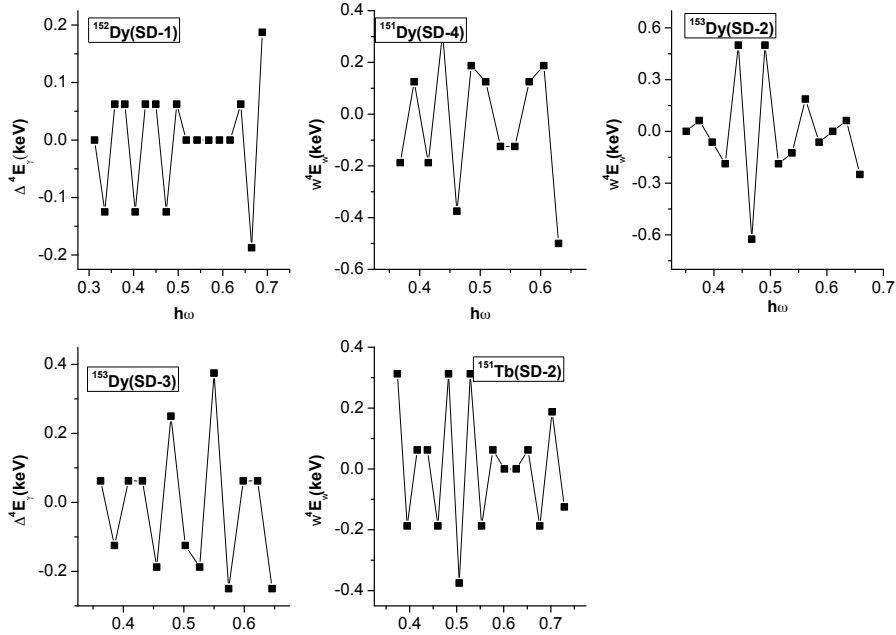


**Figure 6**. $\Delta^4 E_\gamma$ staggering pattern for the $^{152}$Dy(SD-1), $^{151}$Dy(SD-4), $^{153}$Dy(SD-2)(SD-3), and $^{151}$Tb(SD-2).

number increases the staggering also increases. Next result that we are going to discuss is the occurrence of $\Delta I = 2$ staggering effect in the $\gamma$-ray transition energies of $^{152}$Dy(SD-1), $^{151}$Dy(SD-4), $^{153}$Dy(SD-2)(SD-3), and $^{151}$Tb(SD-2) (see Figure 6). In this case, the staggering values lie between $-0.6$ and $0.6$.

Figure 7 shows the variation of staggering index with $\hbar\omega$ for $^{142}$Eu(SD), $^{143}$Eu(SD), $^{144}$Eu(SD-2), and $^{144}$Eu(SD-3). The SD nuclei $^{142}$Eu(SD), $^{143}$Eu(SD), and $^{144}$Eu(SD-3) show large amplitude of staggering index
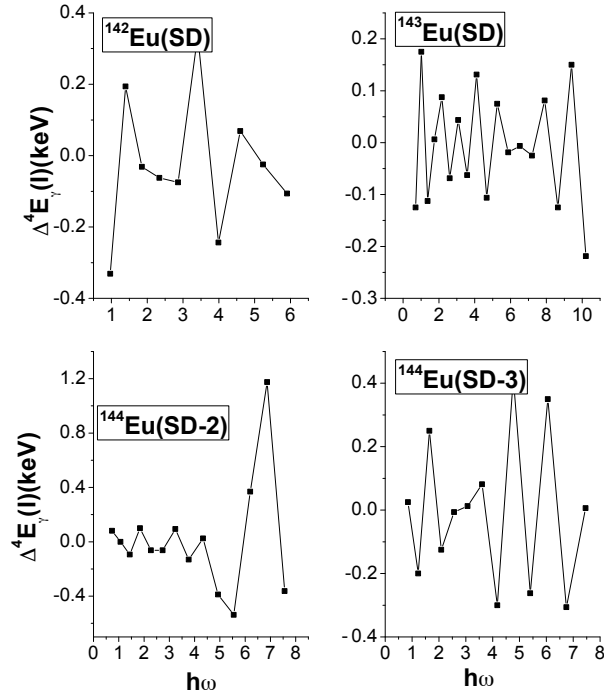
**Figure 7**. $\Delta^4 E_\gamma$ staggering pattern for the $^{142}$Eu(SD), $^{143}$Eu(SD), $^{144}$Eu(SD-2), and $^{144}$Eu(SD-3).
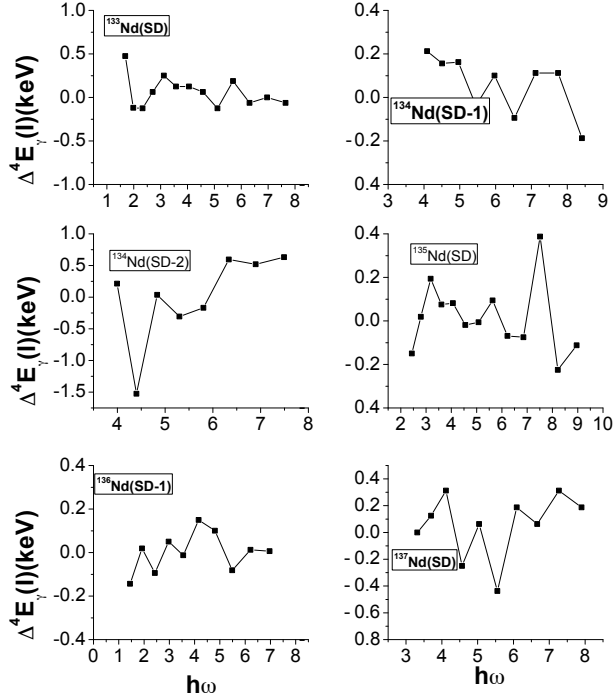


**Figure 8**. $\Delta^4 E_\gamma$ staggering pattern for the $^{133}$Nd(SD), $^{134}$Nd(SD-1), $^{134}$Nd(SD-2), $^{135}$Nd(SD), $^{136}$Nd(SD-1), and $^{137}$Nd(SD).

while $^{144}$Eu(SD-2) shows low amplitude of staggering index at low value of $\hbar\omega$. However, when $\hbar\omega$ increases, the amplitude of staggering index also increases. Figure 8 shows the large amplitude of staggering index for $^{133}$Nd(SD), $^{134}$Nd(SD-1), $^{134}$Nd(SD-2), $^{135}$Nd(SD), $^{136}$Nd(SD-1), and $^{137}$Nd(SD).
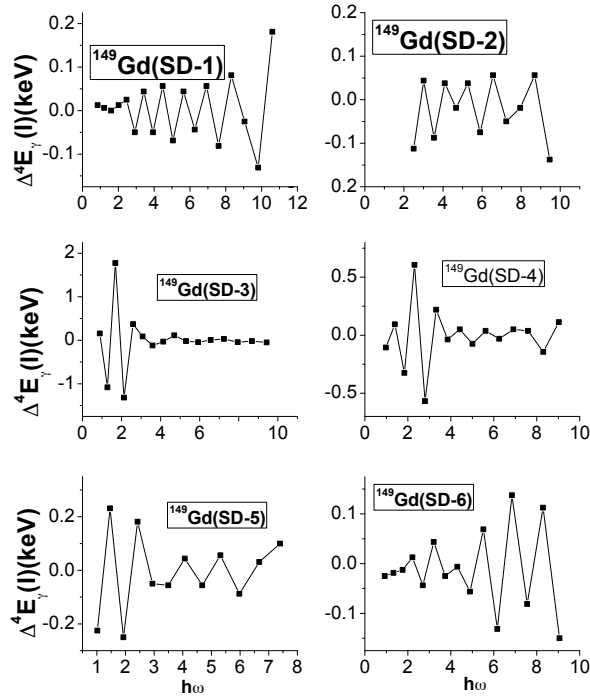
**Figure 9**. $\Delta^4 E_\gamma$ staggering pattern for the $^{149}$Gd(SD-1), $^{149}$Gd(SD-2), $^{149}$Gd(SD-3), $^{149}$Gd(SD-4), $^{149}$Gd(SD-5) and $^{149}$Gd(SD-6).

Similarly, Figure 9 shows the variation of staggering index with $\hbar\omega$ for $^{149}$Gd(SD-1), $^{149}$Gd(SD-2), $^{149}$Gd(SD-3), $^{149}$Gd(SD-4), $^{149}$Gd(SD-5), and $^{149}$Gd(SD-6). The superdeformed bands $^{149}$Gd(SD-1) and $^{149}$Gd(SD-2) have small amplitude of staggering that increases with the increase in $\hbar\omega$. For $^{149}$Gd(SD-3) and $^{149}$Gd(SD-4), the amplitude of staggering is large at initial stage and decreases with the increase in $\hbar\omega$.

Comparison between the predictions of the applied model and the corresponding experimental result is given in Table. The calculated values of *ab* formula and power law for $^{192}$Hg(SD-1) and $^{194}$Hg(SD-1)(SD-2) nuclei are compared with their experimental values and are in good accordance with experimental values. In maximum cases, the deviation from the experimental values is lesser than 10%.

## 3. Conclusion

The above analysis is conducted to understand the implication of identical bands. It seems to be necessary that two truly identical bands must have the same band head moments of inertia. Transition energies of many superdeformed bands were calculated and the nuclear staggering effects within the transitions energies of some superdeformed nuclei were analyzed. The systematic behavior suggests that the band moment of inertia turns out nearly similar for two signature partner bands but the same could not be said for identical SD bands.

## Acknowledgments

**Table**. The calculated and experimental values of band transition for $J+2$ to $J$ for $^{192}$Hg(SD-1), $^{194}$Hg(SD-1) (SD-2), $^{130}$Ce(SD-4), $^{131}$Ce(SD-1), and $^{133}$Ce(SD-1) nuclei.

| Spin | $^{192}$Hg(SD-1) $E_\gamma$(J+2→J) | $ab$ | power | $^{194}$Hg(SD-1) $E_\gamma$(J+2→J) | $ab$ | power | $^{194}$Hg(SD-2) $E_\gamma$(J+2→J) | $ab$ | power |
|---|---|---|---|---|---|---|---|---|---|
| 12 | 300.1 | 300.1 | 301.2 | 296.0 | 296.5 | 295.4 | 283.1 | 282.1 | 280.1 |
| 14 | 341.4 | 340.1 | 339.0 | 337.2 | 338.0 | 337.2 | 323.4 | 324.0 | 325.0 |
| 16 | 381.6 | 382.5 | 384.4 | 416.5 | 415.2 | 417.3 | 363.1 | 360.3 | 366.3 |
| 18 | 421.1 | 423.1 | 425.4 | 454.7 | 453.5 | 451.9 | 402.0 | 401.2 | 405.2 |
| 20 | 458.8 | 455.6 | 459.1 | 491.7 | 490.4 | 488.3 | 440.3 | 443.2 | 443.2 |
| 22 | 496.0 | 496.4 | 498.3 | 527.8 | 526.7 | 525.3 | 477.7 | 480.1 | 479.1 |
| 24 | 532.1 | 531.5 | 534.3 | 562.9 | 561.2 | 561.7 | 514.2 | 513.3 | 516.4 |
| 26 | 567.4 | 569.3 | 568.2 | 596.9 | 595.8 | 593.5 | 549.9 | 547.3 | 548.3 |
| 28 | 601.7 | 604.5 | 603.2 | 630.1 | 629.9 | 626.6 | 584.9 | 582.3 | 586.4 |
| 30 | 634.9 | 632.2 | 629.9 | 662.3 | 660.2 | 663.1 | 619.3 | 616.3 | 623.5 |
| 32 | 668.1 | 666.2 | 667.2 | 693.6 | 691.2 | 695.8 | 652.3 | 650.1 | 655.1 |
| Spin | $^{130}$Ce(SD-4) $E_\gamma$(J+2→J) | $ab$ | power | $^{131}$Ce(SD-1) $E_\gamma$(J+2→J) | $ab$ | power | $^{133}$Ce(SD-1) $E_\gamma$(J+2→J) | $ab$ | power |
| 2 | 1261.0 | 1244.5 | 1230.6 | 590.0 | 575.0 | 556.8 | 748.0 | 733.7 | 712.6 |
| 4 | 2592.0 | 2610.1 | 2619.2 | 1252.0 | 1268.8 | 1270.9 | 1557 | 1572.9 | 1575.1 |
| 6 | 3995.0 | 3988.8 | 4074.5 | 1985.0 | 1979.4 | 2005.7 | 2430.0 | 2424.7 | 2505.0 |
| 8 | 5473.0 | 5371.2 | 5474.8 | 2789.0 | 2695.2 | 2876.8 | 3367.0 | 3280.3 | 3481.5 |
| 10 | 7028 | 7023.8 | 7109.6 | 3663.0 | 3413.3 | 3783.3 | 4370.0 | 4237.7 | 4494.3 |
| 12 | 8662.0 | 8140.1 | 8672.3 | 4606.0 | 4132.5 | 4700.5 | 5438.0 | 5008.9 | 5536.8 |
| 14 | 10379.0 | 95255.0 | 10258.0 | 5617.0 | 5345.0 | 5647.4 | 6570.0 | 6457.8 | 6604.9 |
| 16 | 1216.0 | 11234.0 | 11865.7 | 6698.0 | 6345.8 | 6620.6 | 7768.0 | 7572.8 | 7695.3 |

## References

[1] Strutinsky, V. M. *Nucl. Phys. A* **1968**, *122*, 1-240.

[2] Twin, P. J.; Nyakó, B. M.; Nelson, A. H.; Simpson, J.; Bentley, M. A.; Cranmer-Gordon, H. W.; Forsyth, P. D.; Howe, D.; Mokhtar, A. R.; Morrison, J. D. et al. *Phys. Rev. Lett.* **1986**, *57*, 811-814.

[3] Liang, Y.; Carpenter, M. P.; Janssens, R. V. F.; Ahmad, I.; Henry, R. G.; Khoo, T. L.; Lauritsen, T.; Soramel, F.; Pilotte, S.; Lewis, J. M. et al. *Phys. Rev.C* **1992**, *46*, R2136-R2139.

[4] Nazarewicz, W.; Wyss, R.; Johnson A. *Nucl. Phys. A* **1989**, *503*, 285-330.

[5] Bohr, A.; Mottelson, B. R. *Kgl. Danske Videnskab. Selskab. Mat. -fys. Medd. 27* **1953**, *27*, 16.

[6] Scharff-Goldhaber, G.; Weneser, J. *Phys. Rev.* **1955**, *98*, 212-213.

[7] Wilets L.; Jean, M. *Phys. Rev.* **1956**, *102*, 788-796.

[8] Cizewski, J. A.; Casten, R. F.; Smith, G. J.; Stelts M. L.; Kane, W. R. *Phys. Rev. Lett.* **1978**, *40*, 167-170.

[9] Bohr, A.; Mottelson, B. R. *Nuclear Structure, Vol. II* W. A. Benjamin: New York, NY, USA, 1975.

[10] Holmberg, P; Lipas, P. O. *Nucl. Phys. A* **1968**, *117*, 552-560.

[11] Zeng, G. M.; Zhao, E. G. *Phys.Rev. C* **1995**, *52*, 1864-1870.

[12] von Brentano, P.; Zamfir, N. V.; Casten, R. F.; Rellergert, W. G.; McCutchan, E. A. *Phys. Rev. C* **2004**, *69*, 044314.

[13] Gupta, J. B.; Kavathekar, A. K.; Sharma, R.*Phys. Scr.* **1995**, *51*, 316-321.

[14] Devi, V. *Int. J. Mod. Phy. E* **2015**, *24*, 1550102.

[15] Singh, B.; Zywina, R.; Firestone, R. B. *Nucl. Data Sheets* **2007**, *97*, 241-592.

[16] Twin, P. J. *Nucl. Phys. A* **1990**, *520*, 17c-33c.

[17] Casten, R. F.; Zamfir, N. V.; von Brentano P.; Chou, W. T. *Phys. Rev. C*, **1992** *45*, R1413-R1416.

[18] Casten, R. F. *Phys. Lett. B* **1985**, *152*, 145-276.

[19] Khalaf, A.; Abdelmageed K.; Sirag, M. M. *Turk. J. Phys.* **2013t**, *37*, 49-63.

[20] Khalaf, A. M. ; Taha, M.; Kotob, M. *Prog. Phys.* **2012** *4*, 39-44.

[21] Khalaf, A. M.; Sirag, M. M. *Egypt. J. Phys.* **2004**, *35*, 359-375.

[22] Flibotte, S.; Andrews, H. R.; Ball, G. C.; Beausang, C. W.; Beck, F. A.; Belier, G.; Byrski, T.; Curien, D.; Dagnall, P. J.; France, G. de et al. *Phys. Rev. Lett.* **1993**, *71*, 4299-4302.

[23] Cederwall, B.; Janssens, R. V. F.; Brinkman, M. J.; Lee, I. Y.; Ahmad, I.; Becker, J. A.; Carpenter, M. P.; Crowell, B.; Deleplanque, M. A.; Diamond, R. M. et al. *Phys. Rev. Lett.* **1994**, *72*, 3150-3153.